 DOI: 10.1002/masy.201000084

The Synthesis of Special Block Copolymers Using a Reaction Calorimeter

Nancy Weber,[*1] *John Texter,*[2] *Klaus Tauer*[1]

Summary: The paper provides experimental results about an easy and versatile method to produce amphiphilic block copolymers, block copolymer particles, and even inorganic – polymeric nano-composites via aqueous heterophase polymerization. Special emphasis is placed on the morphology and colloidal properties of some non-ionic di- and triblock copolymer particles with poly(ethylene glycol) of 10^6 g/mol molecular weight as hydrophilic block as well as di-stimuli-responsive block copolymers containing both a poly(N-isopropyl acrylamide) and a poly(ionic liquid) block.

Keywords: block copolymer particles; di–stimuli–responsive block copolymers; heterophase polymerization; reaction calorimeter; silica

Introduction

Reaction calorimetry is an important tool in reaction engineering to accomplish high safety standards in chemical industry, to control lab-scale and industrial production, and to support effectively the transfer of chemical reactions from the laboratory to the industrial scale.[1,2] Reaction calorimetry is also an extremely useful method to follow the kinetics and to develop process models. But reaction calorimetry is even more versatile as effective tool for the synthesis of block copolymers and composite materials via radical heterophase polymerization. It has been successfully applied for the preparation of various multiblock copolymers, of binary composite latex particles of inorganic and polymeric materials, and of di – stimuli - responsive diblock copolymer containing a poly(ionic liquid) as electrolyte and poly(N-isopropyl acrylamide) as thermo-sensitive block.[3–5] The particular benefit of carrying out the synthesis in a reaction calorimeter is that the sequential monomer addition times can be easily and precisely controlled.

The principle of the method is sketched in Figure 1 by means of the combination of two polymerization mechanisms, that is, block copolymer formation via sequential radical polymerization is followed by hydrolytic condensation of one block leading to silica composite block copolymer particles.[4] The method obeys the very general conditions for block copolymer formation via radical polymerization which are a short period of radical formation, an effective reduction of the termination probability, and a sequential monomer addition. Ceric ion redox couples with hydroxymethyl-terminated polymers as reductants fulfill all these requirements. The procedure is versatile and hydrophilic polymers with methylol endgroups are either commercially available such as poly(ethylene glycol) (PEG) or accessible by free radical polymerization with PEG-azo-initiators (PEGA) or 2,2-azobis(2-methyl-N-(2hydroxyethyl)pro-pionamide) (VA-086). Reaction calorimetry is extremely useful to control the conversion of the monomers and to optimize sequential monomer additions.

[1] Max Planck Institute for Colloids and Interfaces, 14476 Potsdam (Golm), Germany
E-mail: Nancy.Weber@mpikg.mpg.de
[2] School of Engineering Technology, Eastern Michigan University, Ypsilanti, MI, 48197, USA

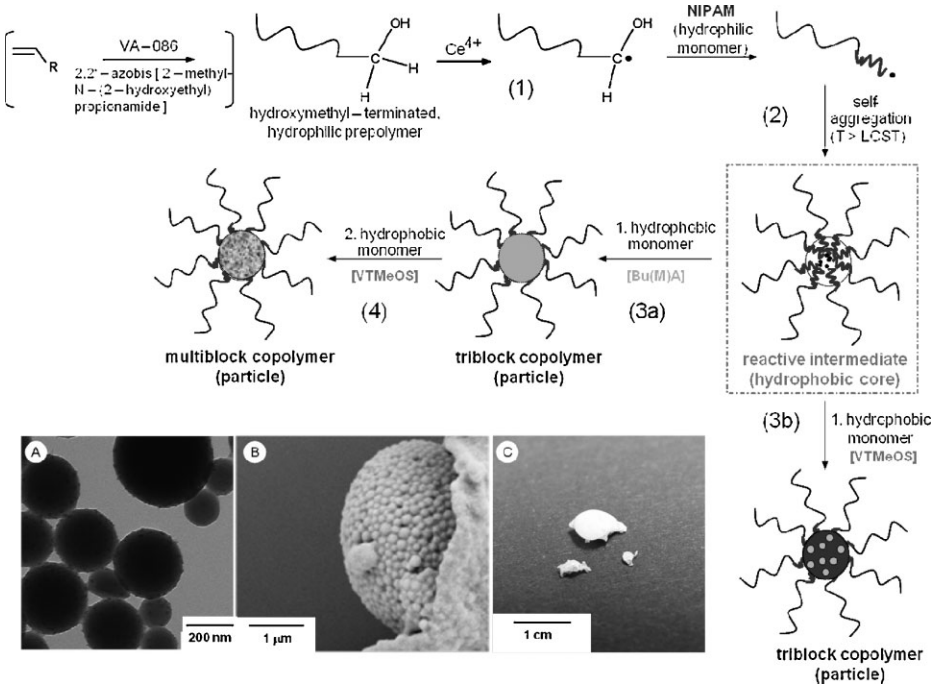

Figure 1.
Illustration of the block copolymer formation protocol via aqueous heterophase layer – by – layer polymerization (drawings not to scale); (1) – water soluble polymer with methylol endgroups, the redox reaction leads to radical formation at the terminal carbon (radical is denoted by the asterisk); (2) NIPAM addition and diblock copolymer formation, the diblock copolymer radicals aggregate if the polymerization temperature is above the lower critical solution temperature (LCST) of the polyNIPAM block, under optimized condition the aggregation practically takes place without termination and leads to diblock copolymer radical particles; (3a, 3b) addition of a hydrophobic monomer leads to triblock copolymer particles with a hydrophobic core, a polyNIPAM middle layer, and a polymeric stabilizer layer; (3b, 4) addition of vinyl trimethoxysilane (VTMeOS) as second hydrophobic monomer creates the conditions for subsequent hydrolytic condensation and silica formation; A-C are images of various states of the PEG-PNIPAM-PVTMeOS triblock copolymer particles (via route 3b): A – TEM image of the redispersed polymer after ultrafiltration and freeze-drying, B – SEM images of the remaining particles after calcinations for 7 hours at 550 °C; C – quartz pearls after burning the solid polymer directly in a high temperature gas flame at 1500 °C.[4]

Experimental Part

Water was taken from a Seral purification system (PURELAB Plus) with a conductivity of 0.06 mS cm^{-1} which was degassed prior to. Styrene and methyl methacrylate (MMA) (all from Aldrich) were distilled under reduced pressure to remove inhibitors and *N*-isopropylacrylamide (NIPAAm, Acros) was carefully recrystallized from a 1:3 volume mixture of toluene / hexane. PEG, mono-methoxy terminated PEG with a molecular weight of 5000 g/mol (mPEG5000, Aldrich), and ceric ammonium nitrate (CAN, Fluka) were used as received. The ionic liquid monomer 1 - (2 - acryloyloxyundecyl)–3–methylimidazolium bromide (IL – Br) was synthesized as described elsewhere[6] and radically polymerized in water with VA-086 initiator (from Wako, used as received) according to standard procedure (5 g of IL-Br, 100 g of water, rotation thermostat). For PIL-1, -2, and -4 the temperature (°C) / initiator amount (mg) was 90 / 250, 67 /125, and 90 / 125, respectively. The expected order of the PIL's molecular weight is PIL-2 > PIL-1 ≥ PIL-4 which was confirmed analytical

ultracentrifugation and size exclusion chromatography in hexafluoro-2-propanol. All block copolymers were synthesized in a CPA200 reaction calorimeter (ChemiSens AB, Lund, Sweden). The water soluble precursor polymer and NIPAM monomer were dissolved in g H_2O and equilibrated to the polymerization temperature. The polymerization was started by adding CAN dissolved in an proper amount of 1 M HNO_3. After the NIPAM polymerization was completed hydrophobic monomers were added, if necessary sequentially. If not otherwise stated the final latexes were purified by ultrafiltration through a YM-100 membrane (regenerated cellulose) with a cut-off of 100 kDa or dialyzed against distilled water until the conductivity of the eluate reached a constant value. The block copolymers were isolated by freeze drying (Beta 1-16, Christ, Germany). The intensity weighted average particle size (D_i) was determined with a Nicomp particle sizer (model 370 or 380, PSS, USA). Transmission and scanning electron microscopy (TEM, SEM) was performed with a Zeiss EM 912 Omega microscope operating at 100 kV and a Leo Gemini 1550 according to standard procedures, respectively. Some samples were characterized with ResoScan URT System (TF Instruments GmbH, Germany) considering the change in the speed of sound with temperature (ΔU versus T) at heating and cooling rate of 300 mK per minute.[7–10] ΔU denotes the difference in the speed of sound in pure water and the sample solution. The URT data are evaluated as temperature derivative of ΔU in dependence on T where the extremum in the dΔU/dT – T curve indicates changes in the water – solute interaction and allows the determination of critical solution temperatures.[7,10]

Results and Discussion

Non-Ionic Block Copolymer Particles

The initiating radicals are generated according to Figure 1 with a PEG of an average molecular weight of one million. Figure 2 illustrates the synthesis by means of calorimetric heat flow – time curves and snapshots of the reaction mixture at different stages of the procedure. There is a significant influence of both the presence of the PNIPAM middle block and the water solubility of the hydrophobic monomer on

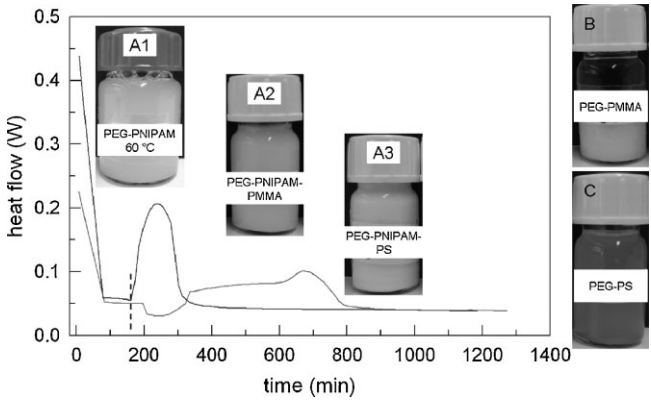

Figure 2.
Smoothed heat flow – time curves (A) and snapshots of triblock copolymer synthesis starting with PEG macroradicals and either MMA or styrene as hydrophobic monomer; the dashed line marks the addition of the hydrophobic monomer and A1 is a snapshot of the reaction mixture at 60 °C showing the PEG-PNIPAM diblock dispersion above the LCST; snapshots A2 and A3 are the final triblock copolymer dispersion PEG-PNIPAM-PMMA and PEG-PNIPAM-PS, respectively; snapshots B and C are the final diblock copolymer dispersion PEG-PMMA and PEG-PS, respectively; recipe: 150 g of water, 1 g of PEG, 0.5 g of NIPAM, 0.548 g of ceric ammonium nitrate, 2 g of styrene or 1.922 g of MMA.

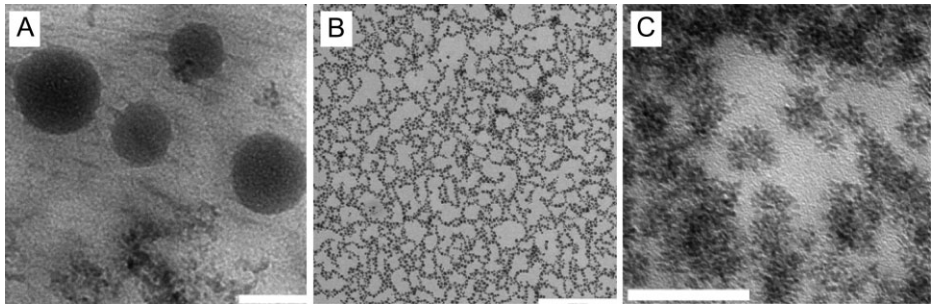

Figure 3.
TEM images showing the precipitation structure of A - PEG with an average molecular weight of one million, B, C – diblock copolymer of PEG-PNIPAM as obtained after the first stage of the polymerization described in Fig. 2 (sample A1); the bar indicates 100, 500, and 50 nm for image A, B, and C, respectively.

the course of the polymerization, the appearance of the block copolymer dispersion, and the particle morphology (cf. Figure 2–4). In the presence of the PNIPAM middle block MMA and styrene can be smoothly polymerized to complete conversion and stable block copolymer dispersions. The calorimeter records reflect a faster polymerization of MMA in accordance with its higher solubility in water. The PEG-PNIPAM precursor particles contain, even above the LCST, quite a high amount of water[8,11] which hinders the diffusion of the more hydrophobic styrene to the radical side and causes the retardation of the polymerization.

Changing the synthetic pathway and omitting the PNIPAM middle block has

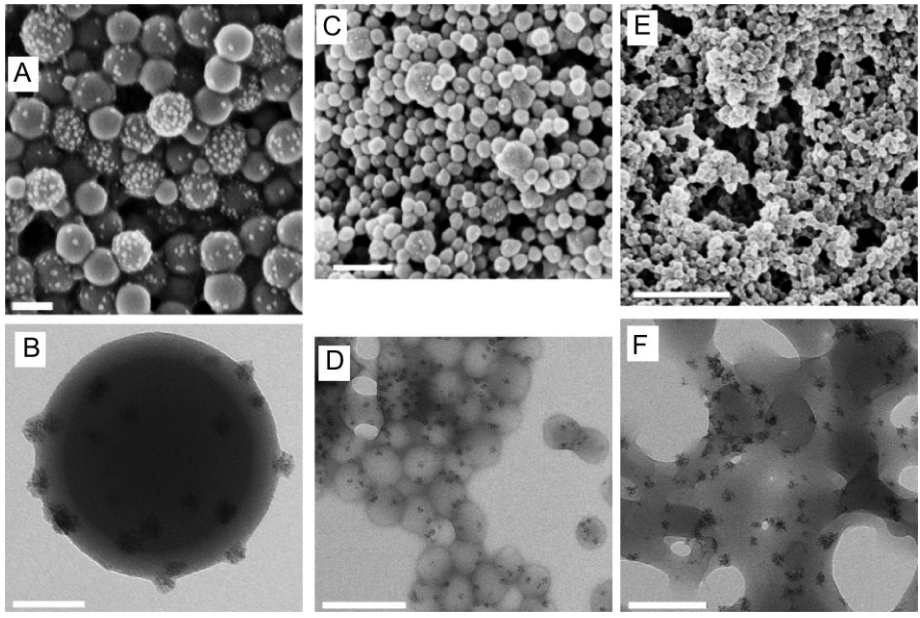

Figure 4.
SEM (A, C, E) and TEM (B, D, F) images of block copolymer particles synthesized as described in Fig. 2; A,B – PEG-PNIPAM-PS bar indicates 200 and 50 nm; C, D - PEG-PNIPAM-PMMA bar indicates 300 and 200 nm; E, F - PEG-PMMA bar indicates 1 μm and 100 nm.

drastic consequences. Under the particular experimental conditions, the conversion of the styrene and MMA polymerization is only 10 and 53%, respectively, again reflecting the difference in the hydrophilicity of both monomers. The PEG-PS copolymer dispersion is only slightly turbid (snapshot C of Figure 2) whereas the PEG-PMMA dispersion separates upon quickly in two phases (cf. snapshot B of Figure 2 showing both phases below and above the label) which, however, are easily redispersable. Expectedly, the morphology of the dried block copolymer particles reflects the different composition and synthetic pathways (cf. Figure 3and 4). Image A of Figure 3 shows a typical precipitation structure of the PEG on TEM grids that consists mainly of both differently shaped and sized isotropic patches. The triblock copolymer particles are of spherical shape and both the SEM and TEM images reveal a peculiar surface morphology (Figure 4 images A, B for PEG-PNIPAM-PS and C, D for PEG-PNIPAM-PMMA). The surface of the particles looks like sprinkled with buds of uniform size between 18 and 20 nm, but the number of (visible) buds per particle differs greatly. The size and shape of the sprinkles is alike the precipitation structure of the PEG-PNIPAM diblock precursor copolymer (image B and C of Figure 3). The structure looks bicontinuous as brighter and darker regions alternate, its size is quite monodisperse, and covers the whole grid. The appearance of the buds is connected with the high molecular weight PEG radicals initiating the polymerization as they are also observed on the PEG-PMMA diblock copolymer particles (image E and F of Figure 4) but have never been seen when using PEG radicals of much lower molecular weight.[4,5]

The observation that the diblock copolymer dispersion (PEG-PMMA), in contrast to the triblock copolymer dispersion (PEG-PNIPAM-PMMA), phase separates is also reflected by the electron microscopy images of Figure 4. Individual particles are clearly to recognize for the triblock copolymer (image C, D) whereas for the diblock copolymer (image E, F) a sponge-like structure is observed. This morphology points to an at least partly compatibility between PEG and PMMA that allows the particles to establish close contact upon drying which is for the triblock copolymers prevented by the middle PNIPAM block. On the other hand, the appearance of the buds proves a partly incompatibility between both polymers, at least for the high molecular weight PEG, which is in context with the controversial discussion in.[12–14]

The observation of the buds that only appear on the particles surface and never isolated on places without particles can be considered as proof for the formation mechanism of this type of amphiphilic block copolymer as discussed. In this sense the buds mark the chain ends of the hydrophilic initiating polymeric radicals and prove aggregative nucleation mechanism sketched in Figure 1.

Di-Stimuli-Responsive Di- and Triblock Copolymers

Also these block copolymers were synthesized according to the procedure outlined in Figure 1 with a hydroxymethyl-terminated poly(1-(2-acryloyloxyundecyl)–3–methylimidazolium bromide) ionic liquid polymer (PIL) as reductant to generate the initiating polymeric radical. After the NIPAM polymerization was completed a part of the reaction mixture was withdrawn from the reactor before styrene or MMA addition.

Both blocks of the PIL-PNIPAM diblock copolymers are stimuli-responsive in a way that the PNIPAM block reacts on temperature changes and the PIL block on the concentration and nature of the counterions as proven newly.[15] The PNIPAM block is hydrophilic below its LCST (app. 32 °C) and it is hydrophobic above the LCST. For the diblock copolymer PIL-PNIPAM, we see that the condensation of the PNIPAM blocks leads to condensation and aggregation above the LCST, but instead of obtaining macrophase separation, we obtain colloidally stable particles,

having PNIPAM cores and stabilizing PIL corona from the diblocks. The anion sensitivity of the PIL blocks suggested we investigate whether high bromide induces condensation. Earlier it was found that poly(ILBr-*co*-MMA) nanolatexes were precipitated by Br^-, BF^{4-}, PF^{6-}, and S^{2-},[6,17] by a mechanism based on imidazolium–anioncondensation, rather than a Debye–Hückel screening effect. We found such an effect in this aqueous diblock system as well. We found the effect of increasing Br– concentration on particle size, and it appears that at a starting diblock concentration, the diblock condenses above a certain Br– concentration. In this system, while the PIL block is condensed, the colloidal stability appears provided by a corona of PNIPAM.[15]

Particularly, the ultrasound resonator technology (URT) is a tool that allows easy investigation of the solution state in dependence on temperature as recently shown for the LCST – behaviour of PNIPAM and PNIPAM block copolymers.[7,10,16] The speed of sound in the sample changes when the interaction between solute and solvent molecules alters in dependence on temperature and the magnitude of the change relates, for a given active solute, to the amount of material involved in the change. Figure 5A shows the results of typical URT experiments with PNIPAM and mPEG5000-PNIPAM block copolymer each at two different concentrations. The extremum of the dΔU/dT – curve is for both polymers between 32 and 33 °C in the range of the LCST of PNIPAM.

Also, the data compared in Figure 6 hold up this conclusion showing a clear correlation between changes of the hydrodynamic diameter and the temperature-derivative of the change in the speed of sound.

For all of the samples, the hydrodynamic diameter increases rapidly exactly at the temperature of the extremum in the dΔU/dT – curve (Figure 6A and C). For the

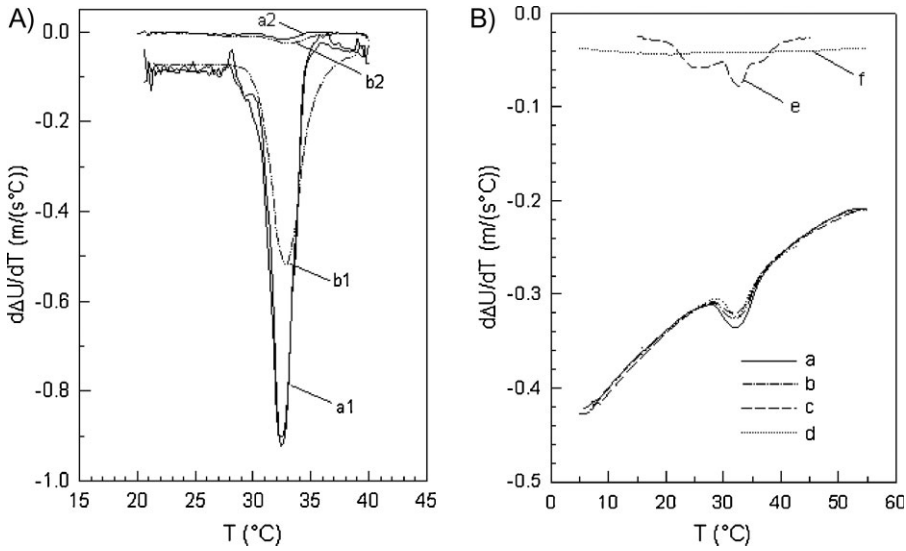

Figure 5.
Temperature derivative of the change in the speed of sound (dΔU/dT) in dependence on temperature for PNIPAM homopolymer, various diblock copolymers, and PIL; Graph A: a1 – two repeats of 1 weight-% aqueous solution of PNIPAM, a2 – 0.025 weight-% aqueous solution of PNIPAM, b1 – 5 weight-% aqueous solution of mPEG5000-PNIPAM diblock copolymer, b2 – 0.25 weight-% aqueous solution of mPEG5000-PNIPAM diblock copolymer; Graph B: PIL-PNIPAM diblock copolymer as obtained after polymerization, a, b – PLI1, c – PIL2, d – PIL4, e – equal molar physical mixture PNIPAM-PIL2, f – PIL2.

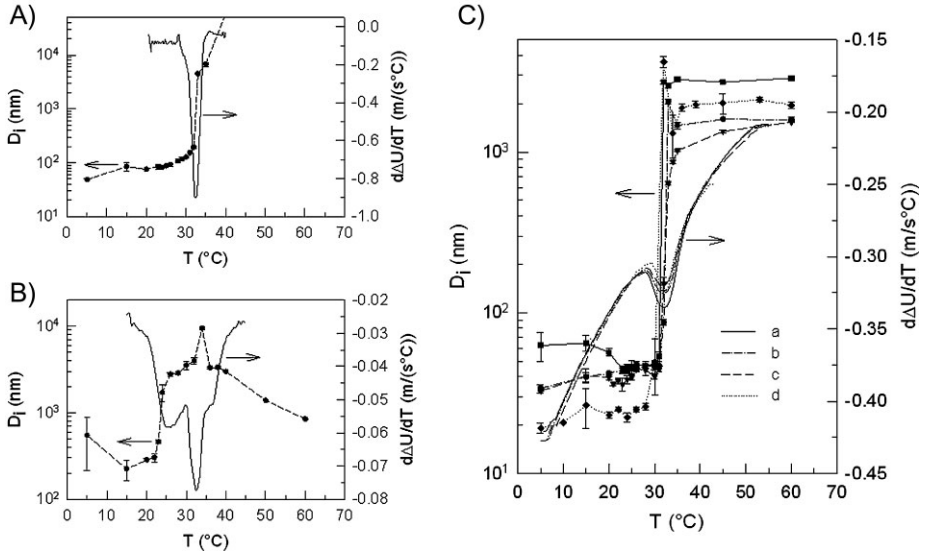

Figure 6.
Comparison of the temperature changes of the average hydrodynamic diameter (D_i symbols and lines) and the temperature derivative of the change in the speed of sound (lines, dΔU/dT); Graph A: PNIPAM, Graph B: equal molar physical mixture PNIPAM-PIL2; Graph C: PIL-PNIPAM diblock copolymer as obtained after polymerization, line a, b and spheres and squares – PLI1, line c and triangles down – PIL2, line d and diamonds – PIL4.

physical mixture the D_i – T curve is a mirror image of the dΔU/dT – dependence which means that the hydrodynamic diameter jumps up already at about 22 °C, that is ten degrees below the PNIPAM LCST but peaks exactly at the LCST of PNIPAM. The temperature dependence of D_i for the PIL (data not shown) posses the expected behavior, almost featureless as anticipated from the URT data (Figure 5B curve 'f') and increasing monotonously due to the increase in the Debye length with increasing temperature. These results show that URT and dynamic light scattering are quite useful complementary methods for the characterization of thermo-sensitive homo- and 'simple' diblock copolymers.

The similarly successful formation of triblock copolymers as described above for the PEG-PNIPAM system (cf. Figure 2) is not possible if the polymerization is started with PIL. The attained conversion with styrene is no more than between 10 and 15% and hence, on electron microscopy images were visibly only few particles. Again, the polymerization of MMA leads to little higher conversion (between 20 and 30%). The low conversion during the polymerization of the hydrophobic monomers with these precursor diblock copolymer particles is caused very likely by the non-optimized conditions as discussed in context with Figure 1 and in.[4]

The position of the thermo-sensitive PNIPAM block in the middle of the triblock copolymer particles, terminated at one end by the hydrophilic PEG or PIL and by the hydrophobic core at the other end, leads to changes in the temperature – dependent properties (cf. Figure 7).

Figure 7A displays dΔU/dT – T curves for the triblock copolymers with styrene. Comparing curve 'a' and 'b' which are almost identical proves the very low conversion of styrene if PIL-PNIPAM precursor was used. Curves 'c, d, e' allow directly to compare the consequences of attaching at both ends of free PNIPAM chains (curve d) successively PEG (curve e) and polystyrene (curve c) on the LCST. Although only one degree the observed changes, in comparison to free PNIPAM,

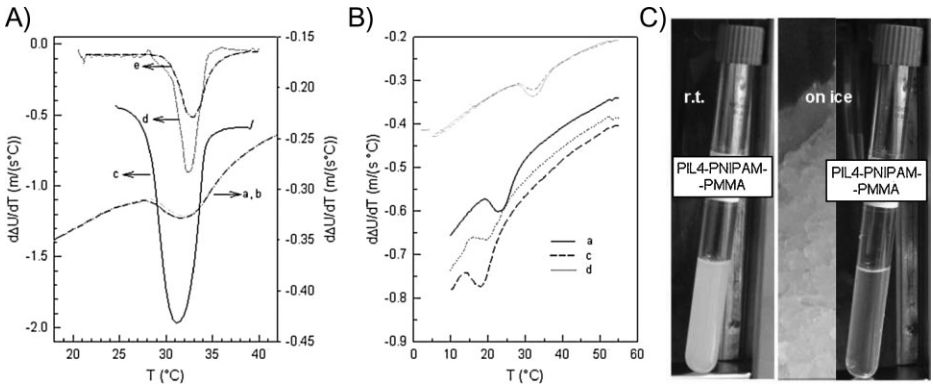

Figure 7.
Thermo-responsive behavior of different triblock copolymer particles as investigated by means of URT; Graph A: polystyrene as hydrophobic block, curve 'a' grey dashed-dotted line – PIL1-PNIPAM diblock copolymer, curve 'b' black dashed-dotted line – PIL1-PNIPAM-PS triblock copolymer, curve 'c' – mPEG5000-PNIPAM-PS triblock copolymer, curve 'd' – PNIPAM homopolymer, curve 'e' – mPEG5000-PNIPAM diblock copolymer; Graph B: PMMA as hydrophobic block, curve 'a' solid line – PIL1-PNIPAM-PMMA, curve 'c' dashed line – PIL4-PNIPAM-PMMA, curve 'd' dotted line – PIL2-PNIPAM-PMMA, the grey curves are the corresponding PIL-PNIPAM diblock copolymers; Graph C: snapshot of the PIL4-PNIPAM-PMMA triblock copolymer dispersion at room temperature (r.t.) and after cooling on ice.

are reasonable. The width of the peak broadens and the LCST is shifted towards higher and lower values for PEG-PNIPAM and PEG-PNIPAM-PS, respectively.

The URT data for the PIL-PNIPAM-PMMA triblocks prove that the LCST is significantly shifted by more than 10 degrees towards lower values and is below room temperature. The snapshots of Figure 7c show the triblock copolymer dispersion (PIL4-PNIPAM-PMMA) at room temperature and after cooling on ice. This great change in the turbidity is surprising but might be explained with the low MMA conversion and hence, quite short hydrophobic blocks which can be disentangled at low temperature, when the greater hydrophilicity of the hydrophilic blocks pulls the chain into water. Nevertheless, the dΔU/dT – curves (Figure 7B) reveal clear differences between the triblock copolymer samples, whose origin is, however, not fully understood at the moment. The need for further studies is additionally supported by the temperature – dependent particle sizes (Figure 8).

Expectedly, the region in the D_i – T curves for the triblock copolymers where strong transitions happen is shifted, in comparison with the diblock copolymers, towards lower temperatures. Also here a gradual change between the triblock copolymers is observed, which is not the case for the diblock precursor copolymers (Figure 8A). Interestingly the transition temperature observed with both completely independent techniques changes in the same order. It is for PIL1-PNIPAM-PMMA > PIL4-PNIPAM-PMMA > PIL2-PNIPAM-PMMA. However, in contrast to the behavior of the diblock copolymers the transition regions determined with both techniques for the triblock copolymers do not coincide. The transition happens in the average particle size – temperature curves at lower temperatures which might be explained with a stepwise segregation / desegregation process. Increasing temperature causes first the aggregation of the most hydrophobic parts, which are the PMMA blocks, with the consequence of increasing hydrodynamic size. The change in the speed of sound reacts particularly on solute – solvent interactions, which is restricted to few Angstrom thick layers of strongly adhering water molecules. The interruption

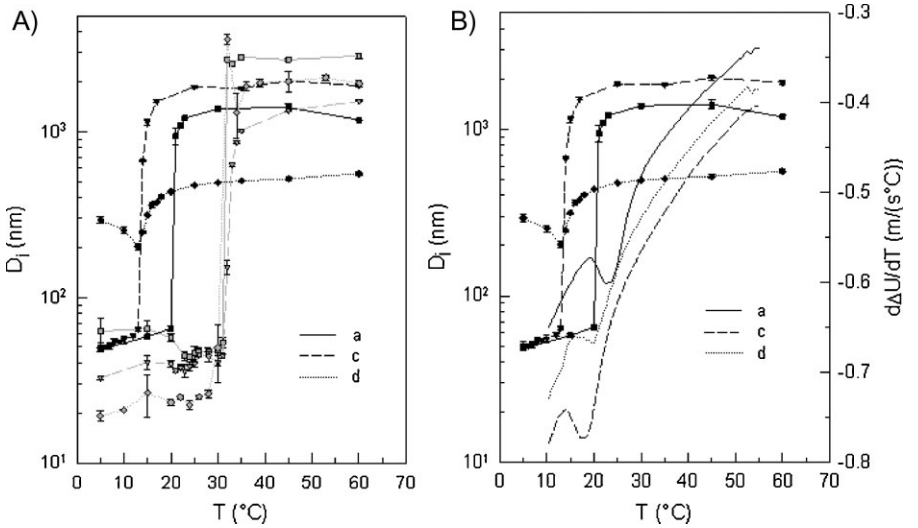

Figure 8.
Thermo-responsive behavior of PIL-PNIPAM-PMMA triblock copolymer particles as investigated by dynamic light scattering and URT; Graph A: change of the hydrodynamic diameter in dependence on temperature; Graph B: Comparison of the temperature changes of the average hydrodynamic diameter (D_i symbols and lines) and the temperature derivative of the change in the speed of sound (lines, $d\Delta U/dT$);, curve 'a' solid line and squares – PIL1-PNIPAM-PMMA, curve 'c' dashed line and triangles down– PIL4-PNIPAM-PMMA, curve 'd' dotted line and diamonds – PIL2-PNIPAM-PMMA, the grey curves and symbols are the corresponding PIL-PNIPAM diblock copolymers.

of the interaction in these layers takes place only at higher temperature requiring closer contact between the chains.

The PIL blocks are sensitive regarding both the concentration and the nature of the anion.[17] Earlier it was found that PIL – co-PMMA nanolatexes were precipitated by Br^-, $BF4^-$, $PF6^-$, and S^{2-}, by a mechanism based on imidazolium – anion condensation, rather than a Debye – Hückel screening effect.[6,17] Such an effect in the PIL-PNIPAM diblock copolymer system was observed as well. It was found that the Br^- concentration had a strong effect on particle size.[15] Particularly, it was detected for PIL2-PNIPAM at a concentration of 1.9 weight-% in water that the diblock condenses above a Br^- concentration of 1.5 M. The images of Figure 9 illustrate the quite enormous influence of the counter ion on the morphology of the triblock copolymer particles. Also in this case the short PMMA blocks allow an easy reorganization of the particles morphology during the experimental steps of the counter ion exchange (cf. caption of Figure 9).

Conclusion

Aqueous radical heterophase polymerization and reaction calorimetry is a powerful combination to produce amphiphilic block copolymers and block copolymer dispersions. Monitoring the whole synthesis in the preparative laboratory scale of about 100 g of overall reaction mass requires high sensitivity calorimeters as the polymerization starts with polymeric radicals and hence, the number of reacting chains is quite low. The use of initiating PEG radicals with a molecular weight as high as 10^6 g/mol allowed the experimental verification of the proposed mechanism of the layer – by – layer construction of block copolymer particles. Due to the quite delicate interplay between aggregative nucleation and radical polymerization

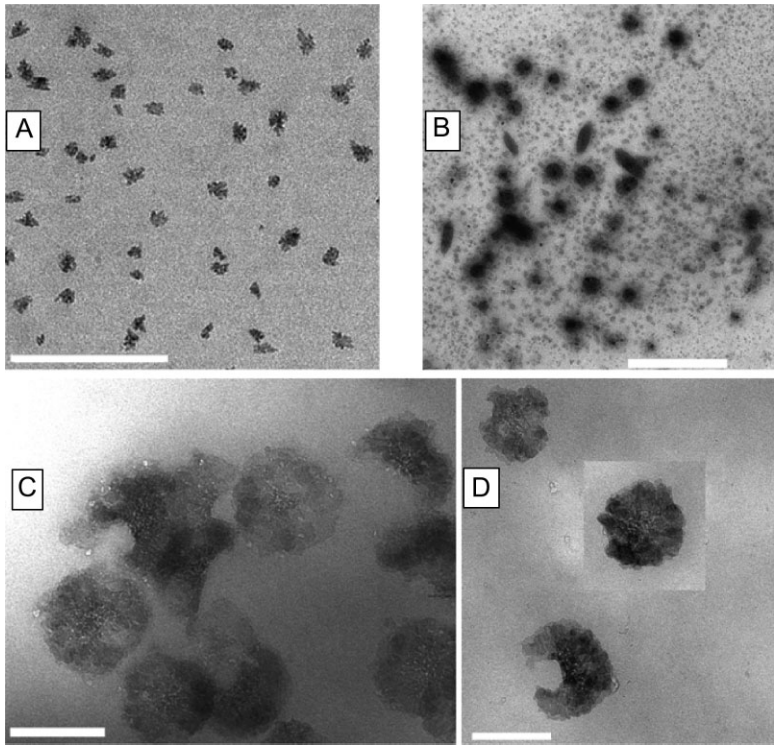

Figure 9.
TEM images illustrating the morphology of different PIL di- and triblock copolymers; A – pre-cipitation structure of PIL-PNIPAM diblocks, bar is 500 nm. B – PIL1(Br^-)-PNIPAM-PMMA tri-block copolymer particles, bar is 500 nm; C, D - PIL1(BF_4^-)-PNIPAM-PMMA triblock copoly-mer particles, bar is 100 and 200 nm for C and D, respectively, PIL1(Br^-)-PNIPAM-PMMA triblock particles were precipitated by excess of $NaBF_4$ and temperature increase. The supernatant was discarded and the precipitate redispersed in water and cooled on ice. This procedure was repeated two times.

kinetics (minimizing radical termination) the conditions needs to be optimized for any combination of blocks, advantageously with reaction calorimetry.

Acknowledgements: We thank Ms. A. Völkel and Dr. Th. Mourey (Eastman Kodak company) for providing us molecular weight estimates for the PIL homopolymers, Ms. U. Lubahn for preparative and analytical assistance, and the MPI of Colloids and Interfaces for financial support.

[1] R. N. Landau, "Expanding the role of reaction calorimetry", *Thermochim. Acta*, **1996**, *289*, 101.
[2] C. LeBlond, J. Wang, R. D. Larsen, C. J. Orella, A. L. Forman, R. N. Landau, J. Laquidara, J. R. Sowa, D. G. Blackmond, Y. K. Sun, "Reaction calorimetry as an in-situ kinetic tool for characterizing complex reactions", *Thermochim. Acta*, **1996**, *289*, 189.
[3] K. Tauer, V. Khrenov, "Polymer dispersions as intermediate state during the synthesis of specialty polymers" *Macromol. Symp.*, **2002**, *179*, 27.
[4] K. Tauer, N. Weber, S. Nozari, K. Padtberg, R. Sigel, A. Stark, A. Volkel, "Heterophase Polymerization as Synthetic Tool in Polymer Chemistry for Making Nanocomposites", *Macromol. Symp.*, **2009**, *281*, 1.
[5] M. D. C. Topp, I. H. Leunen, P. J. Dijkstra, K. Tauer, C. Schellenberg, J. Feijen, "Quasi-living polymerization of N-isopropylacrylamide onto poly(ethylene glycol)", *Macromolecules*, **2000**, *33*, 4986.
[6] D. England, "Materials and Coatings Derived from the Polymerizable Ionic Liquid Surfactant 1-(2-Acryloyloxyundecyl)-3-methylimidazolium Bromide", *MSc thesis*, Eastern Michigan University, Ypsilanti 2008.
[7] K. Tauer, D. Gau, S. Schulze, H. Hernandez, "Transient-thermal and isothermal studies of thermo-sensitive polymer solution with ultrasound resonator technology", *Polymer*, **2008**, *49*, 5452.

[8] K. Tauer, D. Gau, S. Schulze, A. Volkel, R. Dimova, "Thermal property changes of poly(N-isopropylacrylamide) microgel particles and block copolymers", *Coll. Polym. Sci.*, **2009**, *287*, 299.
[9] V. Buckin, C. Smyth, "High-resolution ultrasonic resonator measurements for analysis of liquids", *Sem. Food Anal.*, **1999**, *4*, 113.
[10] K. Van Durme, L. Delellio, E. Kudryashov, V. Buckin, B. Van Mele, "Exploration of high-resolution ultrasonic spectroscopy as an analytical tool to study demixing and remixing in poly(N-isopropyl acrylamide)/water solutions", *J. Polym. Sci. B: Polym Phys.*, **2005**, *43*, 1283.
[11] B. R. Saunders, "*On the structure of poly(N-isopropylacrylamide) microgel particles*", Langmuir, **2004**, *20*, 3925.
[12] S. A. Liberman, A. D. Gomes, E. M. Macchi, "Compatibility in poly(Ethylene oxide)-poly(methyl methacrylate) blends" *J. Polym. Sci. A: Polym. Chem.*, **1984**, *22*, 2809.
[13] T. P. Russell, H. Ito, G. D. Wignall, "Neutron and X-ray-scattering studies on semicrystalline polymer blends", *Macromolecules*, **1988**, *21*, 1703.
[14] K. Tauer, K. Riedelsberger, R. Deckwer, A. Zimmermann, H. Dautzenberg, J. Thieme, "A new way to control particle morphology in heterophase polymerizations", *Macromol. Symp.*, **2000**, *155*, 95.
[15] K. Tauer, N. Weber, J. Texter, "Core-shell particle interconversion with di-stimuli-responsive diblock copolymers", *Chem. Commun.*, **2009**, 6065.
[16] K. Van Durme, G. Van Assche, V. Aseyev, J. Raula, H. Tenhu, B. Van Mele, "Influence of Macromolecular Architecture on the Thermal Response Rate of Amphiphilic Copolymers, Based on Poly(N-isopropylacrylamide) and Poly(oxyethylene), in Water", *Macromolecules*, **2007**, *40*, 3765.
[17] F. Yan, J. Texter, "Surfactant ionic liquid-based microemulsions for polymerization", *Chem. Commun.*, **2006**, 2696.

